Saudi Journal of Biological Sciences (2017) **24**, 1370–1374

King Saud University

Saudi Journal of Biological Sciences

www.ksu.edu.sa
www.sciencedirect.com

ORIGINAL ARTICLE

Characteristics of activated carbon remove sulfur particles against smog

Shengbo Ge [a], **Zhenling Liu** [b], **Yuzo Furuta** [c], **Wanxi Peng** [a,b,*]

[a] *School of Materials Science and Engineering, Central South University of Forestry and Technology, Changsha 410004, China*
[b] *School of Management, Henan University of Technology, Zhengzhou, Henan 450001, China*
[c] *Laboratory of Biomaterials Science, Kyoto Prefectural University, Kyoto, Japan*

Received 16 November 2016; revised 17 December 2016; accepted 18 December 2016
Available online 24 December 2016

KEYWORDS

Activated carbon;
Desulfuration;
Na_2SO_3;
$Na_2S_2O_8$;
Na_2SO_4;
$Fe_2(SO_4)_3$;
S

Abstract Sulfur particles, which could cause diseases, were the main powder of smog. And activated carbon had the very adsorption characteristics. Therefore, five sulfur particles were adsorbed by activated carbon and were analyzed by FT-IR. The optimal adsorption time were 120 min of Na_2SO_3, 120 min of $Na_2S_2O_8$, 120 min of Na_2SO_4, 120 min of $Fe_2(SO_4)_3$ and 120 min of S. FT-IR spectra showed that activated carbon had the eight characteristic absorption of S—S stretch, H_2O stretch, O—H stretch, —C—H stretch, conjugated C═O stretch or C═C stretch, CH_2 bend, C—O stretch and acetylenic C—H bend vibrations at 3850 cm^{-1}, 3740 cm^{-1}, 3430 cm^{-1}, 2920 cm^{-1}, 1630 cm^{-1}, 1390 cm^{-1}, 1110 cm^{-1} and 600 cm^{-1}, respectively. For Na_2SO_3, the peaks at 2920 cm^{-1}, 1630 cm^{-1}, 1390 cm^{-1} and 1110 cm^{-1} achieved the maximum at 20 min. For $Na_2S_2O_8$, the peaks at 3850 cm^{-1}, 3740 cm^{-1} and 2920 cm^{-1} achieved the maximum at 60 min. The peaks at 1390 cm^{-1}, 1110 cm^{-1} and 600 cm^{-1} achieved the maximum at 40 min. For Na_2SO_4, the peaks at 3430 cm^{-1}, 2920 cm^{-1}, 1630 cm^{-1}, 1390 cm^{-1}, 1110 cm^{-1} and 600 cm^{-1} achieved the maximum at 60 min. For $Fe_2(SO_4)_3$, the peaks at 1390 cm^{-1}, 1110 cm^{-1} and 600 cm^{-1} achieved the maximum at 20 min. For S, the peaks at 1630 cm^{-1}, 1390 cm^{-1} and 600 cm^{-1} achieved the maximum at 120 min. It provided that activated carbon could remove sulfur particles from smog air to restrain many anaphylactic diseases.

1. Introduction

Sulfur powder, is solid at room temperature, mainly from the exploitation of natural gas, oil and natural sulfur mine. Reactive sulfur in general, it can burn to sulfur dioxide, mixing with oxidants may explode, can react with the alkali metal (Zhang et al., 2010). An association between high levels of air pollutants and human disease has been known for more than half a century. Air pollution is composed of a heterogeneous mix-

* Corresponding author at: School of Materials Science and Engineering, Central South University of Forestry and Technology, Changsha 410004, China.
E-mail address: pengwanxi@163.com (W. Peng).
Peer review under responsibility of King Saud University.

ELSEVIER Production and hosting by Elsevier

http://dx.doi.org/10.1016/j.sjbs.2016.12.016
1319-562X

ture of compounds including ozone (O_3), carbon monoxide (CO), sulfur dioxide (SO_2), nitrogen oxides (NO_x), liquids, and particulate matter (PM). Substantial epidemiological evidence implicates air pollution, particularly sulfur dioxide (SO_2) and PM, as a major risk factor with serious consequences on human health (Ahmadpour and Do, 1996; Chandra et al., 2009; Jumasiah et al., 2005). Of particular interest in PM are the particles that are $\leqslant$10 μm in diameter (PM_{10}) because they are the PM that ultimately enters the lungs, which may make the person allergic and sick. Globally, the number of people receiving TB therapy grew to 5.4 million in 2013, from 1.0 million enrolled in the DOTS (directly observed treatment, short-course) program in 1995 (Yuan et al., 2004). Sulfur powder and sulfur dioxide (SO_2) often floated in air. If this was inhaled in vivo, it could cause diseases.

Activated carbon can use almost any type of carbon materials, such as wood (Zhang et al., 2010), sawdust, coal (Ding et al., 2002), shells (Yu et al., 2005), the stone of the fruit, bagasse, oil waste, waste plastics (Peng et al., 2014a), paper and leather scrap (Peng et al., 2013a), waste tires, urban waste, etc (Xiao et al., 2013). Activated carbon with highly developed porous structure and huge specific surface area (Peng et al., 2013b), good chemical stability and thermal stability, high mechanical strength and surface contains a variety of oxygen containing functional groups (Wang et al., 2013; Peng et al., 2013c). What's more, activated carbon, which contained potassium, calcium and other minerals, could have adsorption and filtration of extractives, oil, sulfur-based compounds, other matters (Liu et al., 2008; Zhang et al., 2008; Ling et al., 1999; Bautista-Toledo et al., 1994). Therefore, activated carbon has a strong adsorption, and at the same time can make high dispersed catalyst load system, and as a reducing agent to participate in the reaction, reduces the reaction temperature (Wang et al., 2009). Activated carbon adsorption method is simple, no secondary pollution, can be very good for adsorption of sulfide in the air (Lin et al. 2015; Peng et al., 2014b, 2015; Sun et al., 2014; Wang et al., 2009) that was beneficial for people's health. In order to figure out the optimal adsorb condition and the intrinsic change of the activated carbon, five chemicals were adsorbed by activated carbon and were analyzed by FT-IR.

2. Materials and methods

2.1. Materials

Activated carbon, Na_2SO_3, $Na_2S_2O_8$, Na_2SO_4, $Fe_2(SO_4)_3$ and S were purchased from the market.

2.2. Methods

Five kinds of pharmaceutical powders were weighed to 25 g, respectively. These powder and 4 g activated carbon were put into the closed vessel, respectively. It was left in closed vessel for 20 min, 40 min, 60 min, 80 min, 100 min and 120 min, respectively. Each activated carbon was removed, dried, weighed, respectively.

FT-IR spectra: FT-IR spectra of the above samples were obtained using a Thermo Scientific Nicolet iN10 FT-IR microscope as previously mentioned (Lin et al., 2015; Peng et al., 2014b, 2015; Sun et al., 2014; Wang et al., 2009).

3. Result and analysis

Based on the above test, the result of adsorption was obtained and is listed in Table 1.

3.1. SC effect

Based on Table 1, Na_2SO_3's adsorption capacity was 5.01 g/100 g, 9.23 g/100 g, 9.68 g/100 g, 11.9 g/100 g, 11.9 g/100 g, 16.3 g/100 g; $Na_2S_2O_8$'s adsorption capacity was 5.94 g/100 g, 6.93 g/100 g, 12.4 g/100 g, 17 g/100 g, 15.3 g/100 g, 17.7 g/100 g; Na_2SO_4's adsorption capacity was 5.99 g/100 g, 4.24 g/100 g, 5.99 g/100 g, 6.48 g/100 g, 7.54 g/100 g, 15 g/100 g; $Fe_2(SO_4)_3$'s adsorption capacity was 7.21 g/100 g, 6.27 g/100 g, 8.93 g/100 g, 12.1 g/100 g, 13.3 g/100 g, 16.8 g/100 g; S's adsorption capacity was 9.5 g/100 g, 10.2 g/100 g, 11.6 g/100 g, 13.6 g/100 g, 16.8 g/100 g, 19.5 g/100 g for adsorption time of 20 min, 40 min, 60 min, 80 min, 100 min and 120 min, respectively. It showed that adsorption capacity changed at regularity difference. It might be because rapid stirring led to a small amount of five kinds of pharmaceutical powders on the surface of the activated carbon. The optimal adsorption times were 120 min of Na_2SO_3, 120 min of $Na_2S_2O_8$, 120 min of Na_2SO_4, 120 min of $Fe_2(SO_4)_3$ and 120 min of S (Table 2).

3.2. FT-IR analysis

FT-IR spectra were recorded to investigate the functional groups of activated carbon during adsorption of Na_2SO_3, $Na_2S_2O_8$, Na_2SO_4, $Fe_2(SO_4)_3$ and **S**. Spectra of the samples were shown in Figs. 1–5. In the spectrum of adsorption, the S—S stretch, H_2O stretch, O—H stretch, —C—H stretch, conjugated C═O stretch or C═C stretch, CH_2 bend, C—O stretch and acetylenic C—H bend vibrations were observed at 3850 cm^{-1}, 3740 cm^{-1}, 3430 cm^{-1}, 2920 cm^{-1}, 1630 cm^{-1}, 1390 cm^{-1}, 1110 cm^{-1} and 600 cm^{-1}, respectively. For FT-IR spectra of Na_2SO_3, the transmissivity of the peaks at 3850 cm^{-1} and 3740 cm^{-1} achieved the maximum for 120 min, the transmissivity of the peaks at 3430 cm^{-1} and 600 cm^{-1} achieved the maximum for 40 min, the transmissivity of the peaks at 2920 cm^{-1}, 1630 cm^{-1}, 1390 cm^{-1} and 1110 cm^{-1} achieved the maximum for 20 min.

For FT-IR spectra of $Na_2S_2O_8$, the transmissivity of the peaks at 3850 cm^{-1}, 3740 cm^{-1} and 2920 cm^{-1} achieved the maximum for 60 min, the transmissivity of the peaks at 3430 cm^{-1} achieved the maximum for 100 min, the transmissivity of the peaks at 1630 cm^{-1} achieved the maximum for 80 min, the transmissivity of the peaks at 1390 cm^{-1}, 1110 cm^{-1} and 600 cm^{-1} achieved the maximum for 40 min.

For FT-IR spectra of Na_2SO_4, the transmissivity of the peaks at 3850 cm^{-1} and 3740 cm^{-1} achieved the maximum for 40 min, the transmissivity of the peaks at 3430 cm^{-1}, 2920 cm^{-1}, 1630 cm^{-1}, 1390 cm^{-1}, 1110 cm^{-1} and 600 cm^{-1} achieved the maximum for 60 min.

For FT-IR spectra of $Fe_2(SO_4)_3$, the transmissivity of the peaks at 3850 cm^{-1} and 3740 cm^{-1} achieved the maximum for 120 min, the transmissivity of the peaks at 3430 cm^{-1} and

Table 1 Adsorption results.

Adsorption time [min]	20	40	60	80	100	120
Na_2SO_3	5.01	9.23	9.68	11.9	11.9	16.3
$Na_2S_2O_8$	5.94	6.93	12.4	17	15.3	17.7
Na_2SO_4	5.99	4.24	5.99	6.48	7.54	15
$Fe_2(SO_4)_3$	7.21	6.27	8.93	12.1	13.3	16.8
S	9.5	10.2	11.6	13.6	16.8	19.5

Table 2 Groups of activated carbon during adsorption of Na_2SO_3, $Na_2S_2O_8$, Na_2SO_4, $Fe_2(SO_4)_3$ and S (%).

Kind	Peak (cm^{-1})	Adsorption time (min)						Group
		20	40	60	80	100	120	
Na_2SO_3	600	89.8	90.6	89.9	89.3	76.5	87.5	C—H
	1110	90.4	89.0	85.2	87.3	74.8	87.7	C—O stretch
	1390	90.6	89.6	89.3	89.1	78.1	89.3	CH_2 bend
	1630	86.8	86.7	86.2	86.6	75.1	86.2	C═O or C═C
	2920	87.5	87.2	87.3	86.6	76.9	86.8	—C—H stretch
	3430	75.5	78.7	77.5	77.8	64.9	75.9	O—H stretch
	3740	89.2	88.0	87.7	89.3	75.7	90.4	H_2O
	3850	89.4	88.7	88.6	89.6	76.5	90.3	S—S stretch
$Na_2S_2O_8$	600	76.0	91.3	89.9	90.4	87.5	83.7	C—H
	1110	76.1	90.5	89.5	89.3	85.4	83.3	C—O stretch
	1390	76.1	90.5	89.8	89.9	86.7	85.5	CH_2 bend
	1630	73.6	86.9	86.5	87.1	85.5	84.6	C═O or C═C
	2920	72.9	87.1	88.3	87.6	87.6	87.2	—C—H stretch
	3430	63.6	75.7	74.8	75.9	79.9	77.3	O—H stretch
	3740	72.1	89.2	89.9	89.1	88.7	88.8	H_2O
	3850	72.5	89.4	89.5	89.3	89.2	89.0	S—S stretch
Na_2SO_4	600	91.9	88.0	94.1	75.6	70.5	80.7	C—H
	1110	90.0	87.0	92.7	74.4	72.1	81.5	C—O stretch
	1390	90.8	89.1	92.0	75.9	72.6	82.1	CH_2 bend
	1630	86.7	86.0	87.9	73.6	70.7	79.7	C═O or C═C
	2920	87.3	85.4	88.0	73.5	72.4	81.4	—C—H stretch
	3430	75.2	75.0	77.2	64.4	65.1	72.4	O—H stretch
	3740	87.8	89.4	88.3	73.9	71.6	80.8	H_2O
	3850	88.6	89.3	88.8	74.2	72.4	81.6	S—S stretch
$Fe_2(SO_4)_3$	600	93.0	89.8	91.7	90.8	90.8	86.9	C—H
	1110	91.1	88.6	90.3	90.0	89.6	86.2	C—O stretch
	1390	91.6	90.1	91.0	90.2	91.4	88.8	CH_2 bend
	1630	87.5	86.1	88.0	86.8	87.5	86.1	C═O or C═C
	2920	87.0	86.8	87.0	87.4	86.0	85.5	—C—H stretch
	3430	77.6	75.5	77.8	76.4	76.5	75.6	O—H stretch
	3740	87.5	88.0	89.8	89.6	89.5	90.1	H_2O
	3850	88.3	88.7	89.6	89.6	89.6	89.9	S—S stretch
S	600	90.4	87.5	83.3	89.8	88.9	91.7	C—H
	1110	90.9	87.2	84.6	90.2	88.9	90.8	C—O stretch
	1390	90.2	87.4	84.6	90.3	89.5	90.3	CH_2 bend
	1630	86.9	85.9	82.0	87.4	85.8	87.1	C═O or C═C
	2920	88.0	88.0	82.8	88.4	87.0	88.0	—C—H stretch
	3430	77.2	80.4	73.4	77.5	73.7	78.1	O—H stretch
	3740	89.2	88.7	84.5	90.2	89.3	88.4	H_2O
	3850	89.3	89.3	84.3	90.0	89.4	89.1	S—S stretch

1630 cm^{-1} achieved the maximum for 60 min, the transmissivity of the peaks at 2920 cm^{-1} achieved the maximum for 80 min, the transmissivity of the peaks at 1390 cm^{-1}, 1110 cm^{-1} and 600 cm^{-1} achieved the maximum for 20 min.

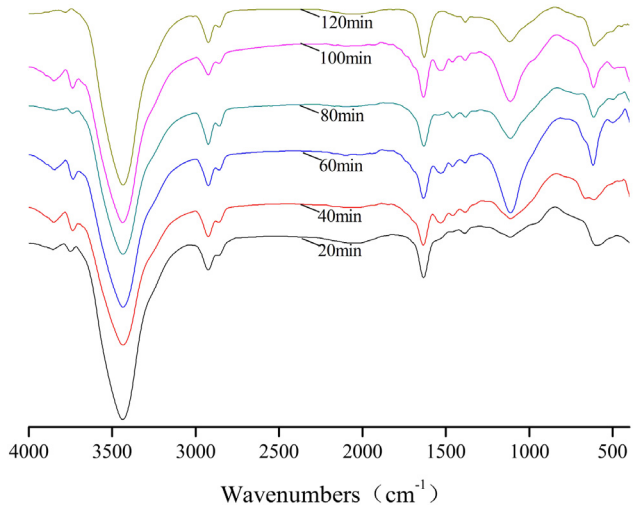

Figure 1 FT-IR spectra of activated carbon during adsorption of Na_2SO_3.

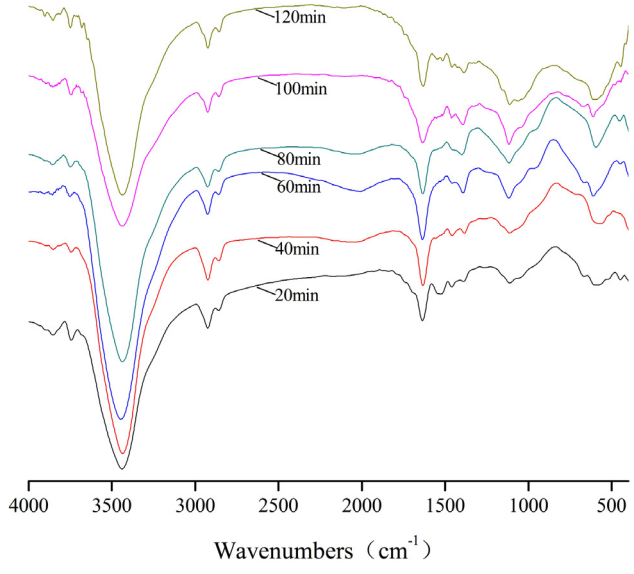

Figure 2 FT-IR spectra of activated carbon during adsorption of $Na_2S_2O_8$.

For FT-IR spectra of S, the transmissivity of the peaks at 3850 cm^{-1}, 3740 cm^{-1} and 2920 cm^{-1} achieved the maximum for 80 min, the transmissivity of the peaks at 3430 cm^{-1} achieved the maximum for 40 min, the transmissivity of the peaks at 1630 cm^{-1}, 1390 cm^{-1} and 600 cm^{-1} achieved the maximum for 120 min, the transmissivity of the peaks at 1110 cm^{-1} achieved the maximum for 20 min.

4. Conclusion

Na_2SO_3's, $Na_2S_2O_8$'s, Na_2SO_4's, $Fe_2(SO_4)_3$'s and S's adsorption capacities were different for adsorption times of 20 min, 40 min, 60 min, 80 min, 100 min and 120 min, respectively. The optimal adsorption times were 120 min of Na_2SO_3, 120 min of $Na_2S_2O_8$, 120 min of Na_2SO_4, 120 min of $Fe_2(SO_4)_3$ and 120 min of S.

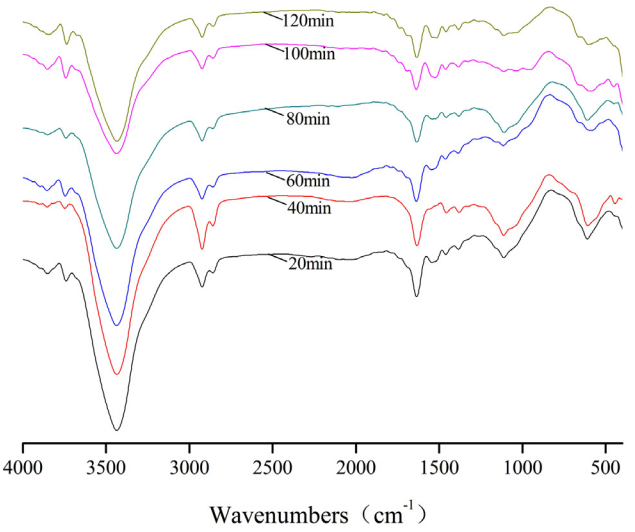

Figure 3 FT-IR spectra of activated carbon during adsorption of Na_2SO_4.

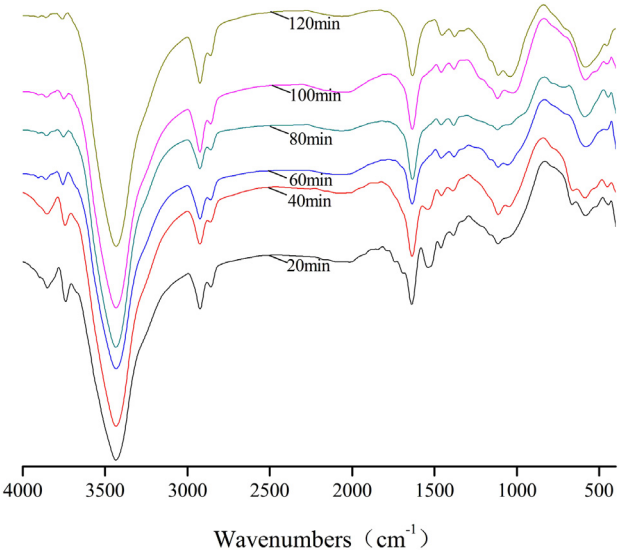

Figure 4 FT-IR spectra of activated carbon during adsorption of $Fe_2(SO_4)_3$.

FT-IR spectra showed that activated carbon had the eight characteristic absorption bands. And the S—S stretch, H_2O stretch, O—H stretch, —C—H stretch, conjugated C═O stretch or C═C stretch, CH_2 bend, C—O stretch and acetylenic C—H bend vibrations were observed at 3850 cm^{-1}, 3740 cm^{-1}, 3430 cm^{-1}, 2920 cm^{-1}, 1630 cm^{-1}, 1390 cm^{-1}, 1110 cm^{-1} and 600 cm^{-1}, respectively. For FT-IR spectra of Na_2SO_3 the transmissivity of the peaks at 2920 cm^{-1}, 1630 cm^{-1}, 1390 cm^{-1} and 1110 cm^{-1} achieved the maximum for 20 min. For FT-IR spectra of $Na_2S_2O_8$, the transmissivity of the peaks at 3850 cm^{-1}, 3740 cm^{-1} and 2920 cm^{-1} achieved the maximum for 60 min the transmissivity of the peaks at 1390 cm^{-1}, 1110 cm^{-1} and 600 cm^{-1} achieved the maximum for 40 min. For FT-IR spectra of Na_2SO_4, the transmissivity of the peaks at 3430 cm^{-1}, 2920 cm^{-1}, 1630 cm^{-1}, 1390 cm^{-1}, 1110 cm^{-1} and 600 cm^{-1} achieved the maximum for 60 min.

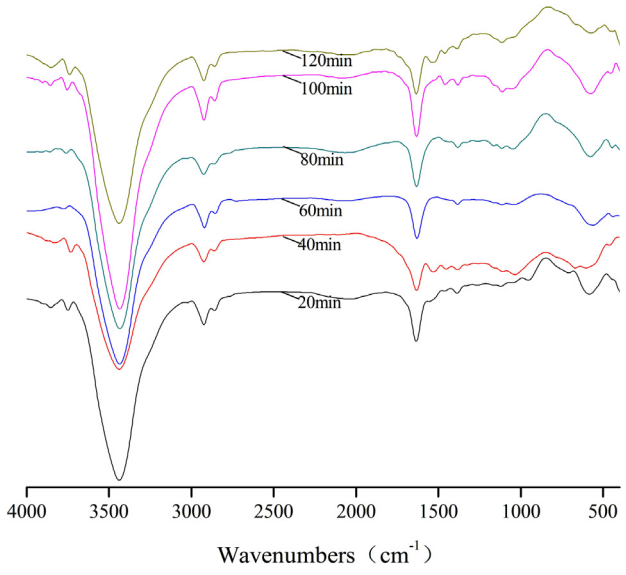

Figure 5 FT-IR spectra of activated carbon during adsorption of S.

For FT-IR spectra of $Fe_2(SO_4)_3$, the transmissivity of the peaks at 1390 cm^{-1}, 1110 cm^{-1} and 600 cm^{-1} achieved the maximum for 20 min. For FT-IR spectra of S, the transmissivity of the peaks at 1630 cm^{-1}, 1390 cm^{-1} and 600 cm^{-1} achieved the maximum for 120 min. In these states, the number of the transmissivity of the maximum peaks is the largest.

Acknowledgment

This work was financially supported by the National 948 Plan (2014-4-38).

References

Ahmadpour, A., Do, D.D., 1996. The preparation of activated carbon from coal by chemical and physical activation. Carbon 34, 471–479.

Bautista-Toledo, I., Rivera-Utrilla, J., Ferro-Garcia, M.A., MORENO-Castilla, C., 1994. Influence of the oxygen surface complexes of activated carbons on the adsorption of chromium ions from aqueous solutions: effect of sodium chloride and humic acid. Carbon 32, 93–100.

Chandra, T.C., Mirna, M.M., Sunarso, J., et al, 2009. Activated carbon from durian shell: preparation and characterization. J. Taiwan Inst. Chem. E. 40, 457–462.

Ding, L.P., Bhatia, S.K., Liu, K., 2002. Kinetics of adsorption on activated carbon: application of heterogeneous vacancy solution theory. Chem. Eng. Sci. 57, 3909–3928.

Jumasiah, A., Chuah, T.G., Gimbon, J., et al, 2005. Adsorption of basic dye onto palm kernel shell activated carbon: sorption equilibrium and kinetics studies. Desalination 186, 57–64.

Ling, L., Li, K., Miyamoto, S., Korai, Y., Kawano, S., et al, 1999. Removal of SO_2 over ethylene tar and cellulose based active carbon filter. Carbon 37, 499–504.

Liu, Q.M., Luo, Y.S., Yin, S.P., Chen, S.M., Zhang, D.Q., Peng, W. X., 2008. Liquid rheology study on refined rapeseed oil. J. Cent. South Univ. T. 15, 525–528.

Peng, W.X., Lin, Z., Chang, J.B., Gu, F.L., Zhu, X.W., 2013a. Biomedical molecular characteristics of YBSJ extractives from *Illicium verumfruit*. Biotechnol. Biotec. Eq. 27, 4311–4316.

Peng, W.X., Wang, L.S., Lin, Z., Minglong Zhang, M.L., 2013b. Identification and chemical bond characterization of wood extractives in three species of eucalyptus biomass. J. Pure Appl. Microbiol. 7, 67–73.

Peng, W.X., Wang, L.S., Zhang, M.L., Lin, Z., 2013c. Molecule characteristics of eucalyptus hemicelluloses for medical microbiology. J. Pure Appl. Microbiol. 7, 1345–1349.

Peng, W.X., Ge, S.B., Li, D.L., Mo, B., Daochun, Q., Ohkoshi, M., 2014a. Molecular basis of antibacterial activities in extracts of *Eucommia ulmoides* wood. Pak. J. Pharm. Sci. 27, 2133–2138.

Peng, W.X., Wang, L.S., Zhang, M.L., Lin, Z., 2014b. Separation characteristics of lignin from *Eucalyptus camaldulensis* lignincelluloses for biomedical cellulose. Pak. J. Pharm. Sci. 27, 723–728.

Peng, W.X., Lin, Z., Chen, H., et al, 2015. Biochemical group characteristics of self-bonded boards during acidic oxidation for public health. J. Pure Appl. Microbiol. 9, 307–311.

Sun, Y.C., Lin, Z., Peng, W.X., et al, 2014. Chemical changes of raw materials and manufactured binderless boards during hot pressing: lignin isolation and characterization. Bioresources 9, 1055–1071.

Wang, Z.Z., Lv, P., Hu, Y., Hu, K.L., 2009. Thermal degradation study of intumescent flame retardants by TG and FTIR: melamine phosphate and its mixture with pentaerythritol. J. Anal. Appl. Pyrol. 86, 207–214.

Wang, L.S., Peng, W.X., Zhang, M.L., Lin, Z., 2013. Separation characteristics of lignin from eucalyptus lignincellulose for medicinal biocellulose preparation. J. Pure Appl. Microbio. 7, 59–66.

Xiao, Z.P., Peng, Z.Y., Dong, J.J., et al, 2013. Synthesis molecular docking and kinetic properties of beta-hydroxy-beta-phenylpropionyl-hydroxamic acids as *Helicobacter pylori* urease inhibitors. Eur. J. Med. Chem. 68, 212–221.

Yu, G.X., Lu, S.X., Chen, H., et al, 2005. Diesel fuel desulfurization with hydrogen peroxide promoted by formic acid and analyzed by activated carbon. Carbon 43, 2285–2294.

Yuan, C.S., Lin, H.Y., Wu, C.H., et al, 2004. Preparation of sulfurized powdered activated carbon from waste tires using an innovative compositive impregnation process. J. Air Waste Manage. 54, 862–870.

Zhang, D.Q., Chen, S.M., Peng, W.X., et al, 2008. Rheology study of supercritically extracted tea-oil. J. Cent. South Univ. T. 15, 506–508.

Zhang, H.P., Yan, Y., Yang, L.C., 2010. Preparation of activated carbon from sawdust by zinc chloride activation. Adsorption 16, 161–166.